Clin Orthop Relat Res (2009) 467:651–659
DOI 10.1007/s11999-008-0617-5

SYMPOSIUM: FEMOROACETABULAR IMPINGEMENT: CURRENT STATUS OF DIAGNOSIS AND TREATMENT

Do Normal Radiographs Exclude Asphericity of the Femoral Head-Neck Junction?

Marcel Dudda MD, Christoph Albers MD, Tallal Charles Mamisch MD, Stefan Werlen MD, Martin Beck MD

Published online: 20 November 2008

Abstract Asphericity of the femoral head-neck junction is one cause for femoroacetabular impingement of the hip. However, the asphericity often is underestimated on conventional radiographs. This study compares the presence of asphericity on conventional radiographs with its appearance on radial slices of magnetic resonance arthrography (MRA). We retrospectively reviewed 58 selected hips in 148 patients who underwent a surgical dislocation of the hip. To assess the circumference of the proximal femur, alpha angle and height of asphericity were measured in 14 positions using radial slices of MRA. The hips were assigned to one of four groups depending on the appearance of the head-neck junction on anteroposterior pelvic and lateral crosstable radiographs. Group I (n = 19) was circular on both planes, Group II (n = 19) was aspheric on the crosstable view, Group III (n = 4) was aspheric on the anteroposterior view, and Group IV (n = 13) was aspheric on both views. In all four groups, the highest alpha angle was found in the anterosuperior area of the head-neck junction. Even when conventional radiographs appeared normal, an increased alpha angle was present anterosuperiorly. Without the use of radial slices in MRA, the asphericity would be underestimated in these patients.
Level of Evidence: Level II, prognostic study. See the Guidelines for Authors for a complete description of levels of evidence.

Introduction

Femoroacetabular impingement (FAI) is an accepted cause of early osteoarthrosis (OA) of the hip [2, 6, 8, 11, 12]. FAI describes a pathologic abutment between the femoral head and the acetabular rim. Two basic mechanisms, cam and pincer FAI, are responsible for the cartilage damage [2, 6, 8]. However, isolated pincer or cam FAI is rare; most often a combination of both is present [2]. Pincer FAI is secondary to general or local overcoverage of the acetabulum. Cartilage damage is restricted to a narrow streak along the acetabular rim. Cam FAI is secondary to an aspheric extension of the cartilage-bearing area of the femoral head onto the neck [23]. Depending on the location, the aspheric part is squeezed into the acetabulum during flexion of the hip or during a combination of flexion and internal, occasionally external, rotation of the hip. The acetabular articular cartilage is pushed away from the rim, creating initial softening of the acetabular cartilage and later disconnection from the labrum and subchondral bone with flap formation. Cartilage damage can be substantial at early stages of the disease and can involve up to ⅓ of the depth of the acetabular cartilage, measured for the rim towards the center of the acetabulum [2].

Deformities of the acetabulum (coxa profunda, protrusio, retroversion) are easily recognized on standardized radiographs of the hip [22]. Alterations of the head-neck

Each author certifies that he has no commercial association (eg, consultancies, stock ownership, equity interest, patent/licensing arrangements, etc) that might pose a conflict of interest in connection with the submitted article.
Each author certifies that his or her institution has approved the human protocol for this investigation and that all investigations were conducted in conformity with ethical principles of research.

M. Dudda (✉), C. Albers, T. C. Mamisch, M. Beck
Department of Orthopaedic Surgery, Inselspital, University of Berne, Freiburgstrasse, 3010 Bern, Switzerland
e-mail: Marcel.Dudda@rub.de

S. Werlen
Department of Radiology, Hospital Sonnenhof, Bern, Switzerland

junction, however, are overlooked easily, because they are often subtle and located at the anterosuperior aspect of the femoral head [17]. For diagnosis and surgical treatment with surgical hip dislocation or hip arthroscopy, it is necessary to verify the exact position of the bone deformity [5, 7]. Standard radiographs like anteroposterior pelvis and crosstable views are the gold standard in first step diagnostics of cam-type FAI [17]. Several authors recommend different radiographic views to detect the bone deformity. Some prefer crosstable views and others special projections like Dunn 45° view or frog-leg lateral view [3, 4, 17]. However, to examine the circumference of the femoral head-neck junction, the most accurate imaging is magnetic resonance arthrography (MRA) with radial slices (MR slice planes all containing the femoral neck axis near the femoral head-neck junction) [13–16, 19]. In this sequence, the slices are positioned in a clockwise way around the axis of the femoral neck.

In contemporary joint-preserving hip surgery, the surgical correction of these anatomic abnormalities aims to prevent or at least decelerate the development of secondary OA [5]. However, diagnosis and treatment is only possible if surgeons exactly know where to look for the abnormalities.

We hypothesized (1) the asphericity of the head-neck junction sometimes is missed in regular radiographs; (2) the asphericity of the femoral head is underestimated if standard radiographs are normal; (3) that MRA with radial slices are superior to regular radiographs to visualize osseous abnormalities.

Materials and Methods

We retrospectively reviewed the radiographs of the affected side of all 148 patients who underwent surgical dislocation of the hip for the treatment of FAI from 2005 to 2007. We classified the femoral head asphericity into four groups. A circle was drawn around the femoral head in the anteroposterior pelvis and lateral crosstable views. The head-neck transition was considered spherical if the transition from the femoral head to the neck was contained within the circle (Figs. 1A, B, 2A, B). Group I (n = 19) included hips with spherical contours on both the anteroposterior pelvis and lateral crosstable views (Fig. 1A–B). Group II (n = 19) included hips with asphericity on the lateral crosstable view only. Group III (n = 4) had asphericity of the hip on the anteroposterior pelvis (eg, pistol grip deformity) but was normal in the lateral crosstable view. Group IV (n = 13) included hips with aspheric head-neck junction on both views (Fig. 2A, B). We excluded 52 of the 148 hips with Tönnis Stage 1

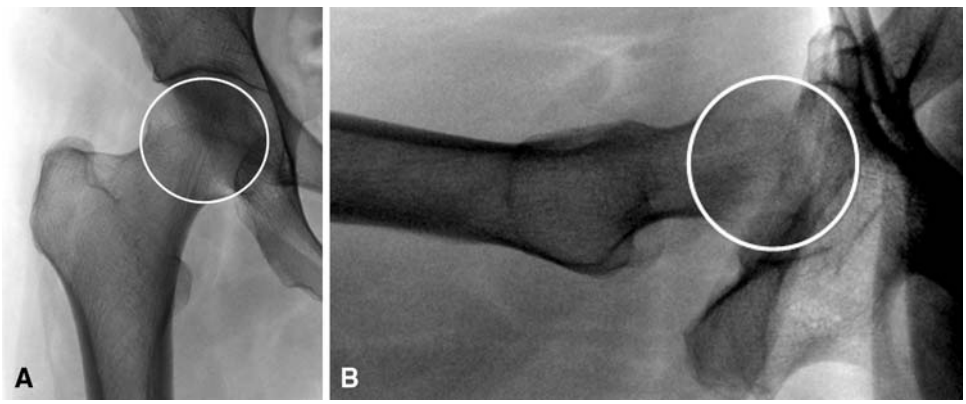

Fig. 1A–B (**A**) Anteroposterior pelvis view of a patient without radiographic signs of femoroacetabular impingement (Group I). (**B**) Lateral crosstable view of a patient without radiographic signs of femoroacetabular impingement (Group I).

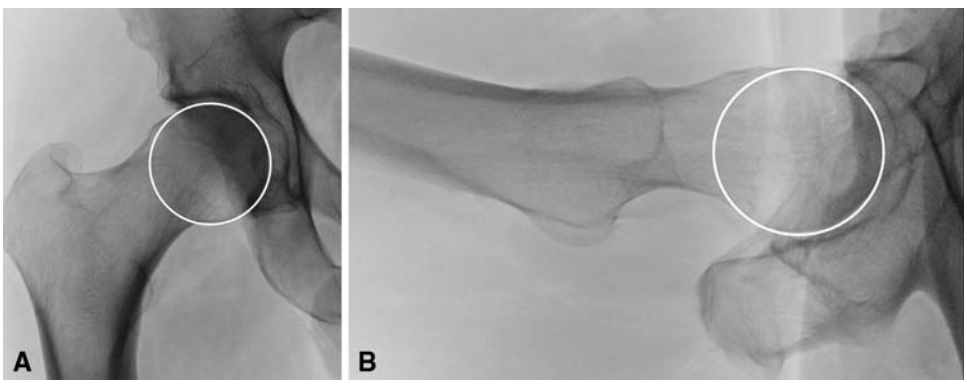

Fig. 2A–B (**A**) Anteroposterior pelvis view of a patient with radiographic signs of femoroacetabular impingement in both planes (Group IV). (**B**) Lateral crosstable view of a patient with radiographic signs of femoroacetabular impingement in both planes (Group IV).

Fig. 3 Construction of the alpha angle as described by Nötzli et al. [18].

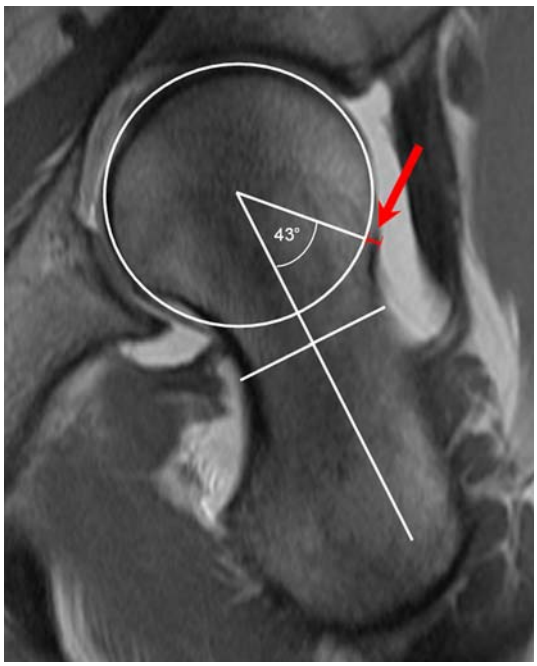

Fig. 4 Magnetic resonance arthrogram slice of radial slices showing the measurement of the height of asphericity at an alpha angle of 43°.

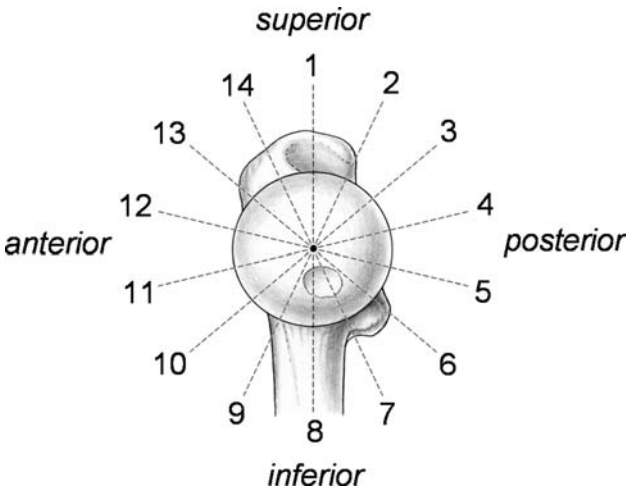

Fig. 5 Schematic of the proximal femur showing the clockwise rotation of the MRI slices, in which measurements were taken.

osteoarthrosis [24] and higher and 41 because of MRAs without radial slices, incomplete radiographic documentation, or MRAs not performed with the technique described subsequently. The remaining 55 hips were included in the study. Mean age of the patients was 33.8 years (range, 16.7–53.7 years).

We (CA, MD) measured the shape of the femoral head-neck junction using the radial slices of the MRA in 14 cuts around the femoral head-neck. At each position, the angle alpha was measured analogous to the technique described previously (Fig. 3) [18]. We measured the height of the asphericity at an angle alpha of 43° to obtain an idea of the magnitude of the deformity (Fig. 4). Based on the data of previous works by Nötzli et al. [18] and Beaulé et al. [1], an alpha angle of 43° was considered normal. All data were converted to a right hip to allow comparison and analysis.

Standardized conventional anteroposterior and axial pelvic radiographs were performed as described previously [21]. We (CA,MD) determined the presence or absence of osseous bumps in the different groups, acetabular retroversion (crossover sign) [20], coxa profunda, protrusio acetabuli, the lateral center edge angle [27], and the acetabular slope [25].

MRA was performed on a 1.5-Tesla high-field scanner (Siemens, Erlangen, Germany) using a flexible surface body coil for high spatial resolution. We injected 10 to 20 mL of saline-diluted gadolinium DTPA (Dotarem 1:200; Guebert AG, Paris, France) intraarticularly under fluoroscopic guidance. In addition to the standard MRI protocol, radial proton density-weighted sequences (TR 2000, TE 15, 260 × 260-mm field of view, 266 x 512 matrix, 4-mm section thickness, 16 slices, 4 minutes 43 seconds) were oriented along the axis of the femoral neck (Fig. 5). The images were performed (Fig. 6A–G) based on a sagittal oblique localizer (Fig. 6H), marked on the proton density-weighted coronal sequence.

Results

Of the 55 hips analyzed, 41 had acetabular retroversion with a positive crossover sign, 34 had mixed-type

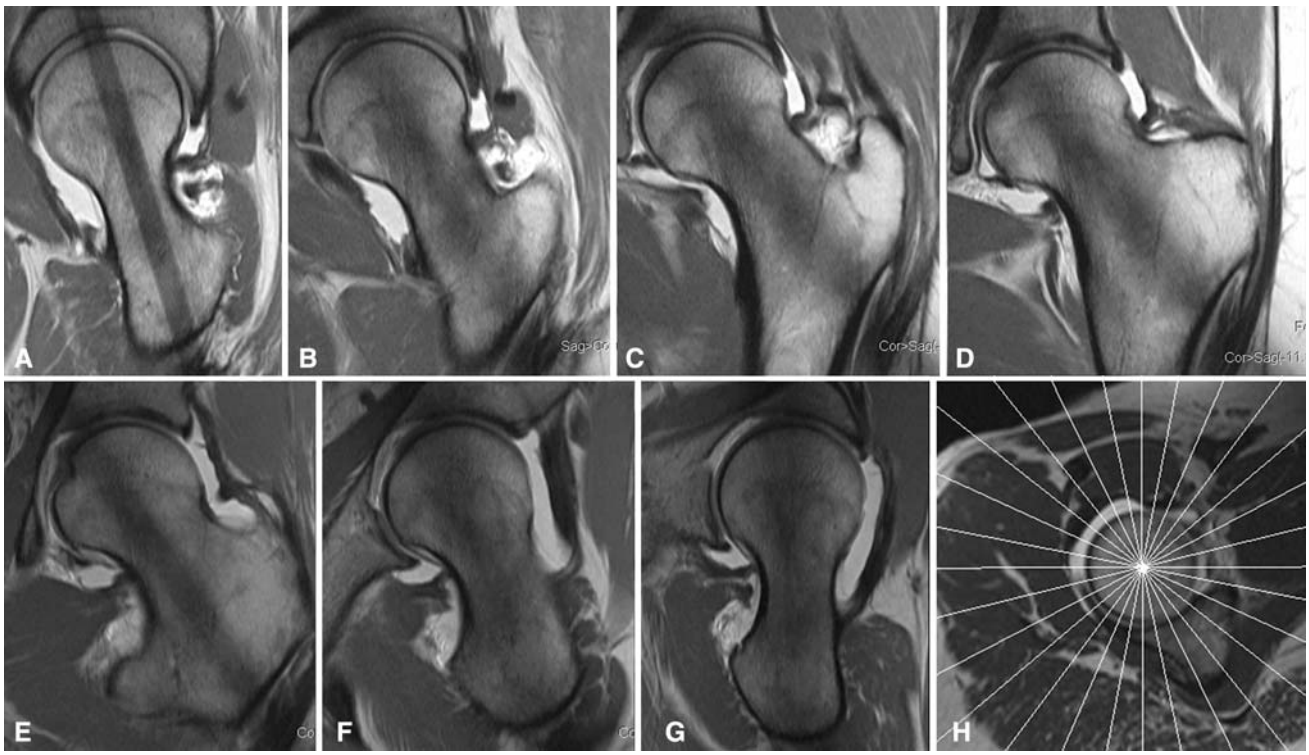

Fig. 6A–H (**A**) Example of a MRA radial slice at 3 o'clock position (posterior) at the femoral neck axis. (**B**) Example of a MRA radial slice at 2 o'clock position at the femoral neck axis. (**C**) Example of a MRA radial slice at 1 o'clock position at the femoral neck axis. (**D**) Example of a MRA radial slice at 12 o'clock position (superior) at the femoral neck axis. (**E**) Example of a MRA radial slice at 11 o'clock position at the femoral neck axis. (**F**) Example of a MRA radial slice at 10 o'clock position at the femoral neck axis. (**G**) Example of a MRA radial slice at 9 o'clock position (anterior) at the femoral neck axis. (**H**) Magnetic resonance arthrogram radial slice localizer.

Table 1. Alpha angles and height of asphericity for each group with equivalent times in clockwise rotation

Group	Alpha angle (degrees)		Maximum height of asphericity (mm)
	Highest	Lowest	
Group I— no radiographic signs of FAI	56.2 (10 o'clock)	40.1 (4 o'clock)	2.8 (11 o'clock)
Group II—radiographic signs of FAI only on lateral crosstable view	61.4 (11 o'clock)	42.2 (4 o'clock)	3.3 (10 o'clock)
Group III—radiographic signs of FAI only on anteroposterior pelvis view	73.1 (7 o'clock)	45.9 (3 o'clock)	2.8 (10 o'clock)
Group IV—radiographic signs of FAI on anteroposterior pelvis view and on lateral crosstable view	66.2 (12 o'clock)	39.6 (8 o'clock)	4.5 (12 o'clock)

impingement with coxa profunda, and 21 had isolated cam-type impingement. The center edge angle averaged 30.1° (range, 14.6°–51.5°) and the acetabular roof angle was 7.1° (range, −5°–21.8°).

Based on the radiographic appearance of the head sphericity on the anteroposterior pelvis and lateral crosstable views, 19 hips were in Group I with spherical head-neck junctions in both planes, 19 hips in Group II with asphericity in the axial view, four hips in Group III with asphericity only in the anteroposterior view, and 13 hips in Group IV with an aspheric head-neck junction on both anteroposterior pelvis and lateral crosstable views.

The mean lateral center edge angle in Group I was 30.1° (range, 18°–39.5°), in Group II 31.5° (range, 23.2°–51.5°), in Group III 29.7° (range, 29.7°–40.2°), and in Group IV 24.4° (range, 14.6°–32.4°). The mean acetabular slope in Group I was 6.3°, in Group II 7.1°, in Group III 7.2°, and in Group IV it was 8.2°.

In all groups, the alpha angle was increased anterosuperiorly between Slice 12 (9 o'clock) and Slice 1 (12

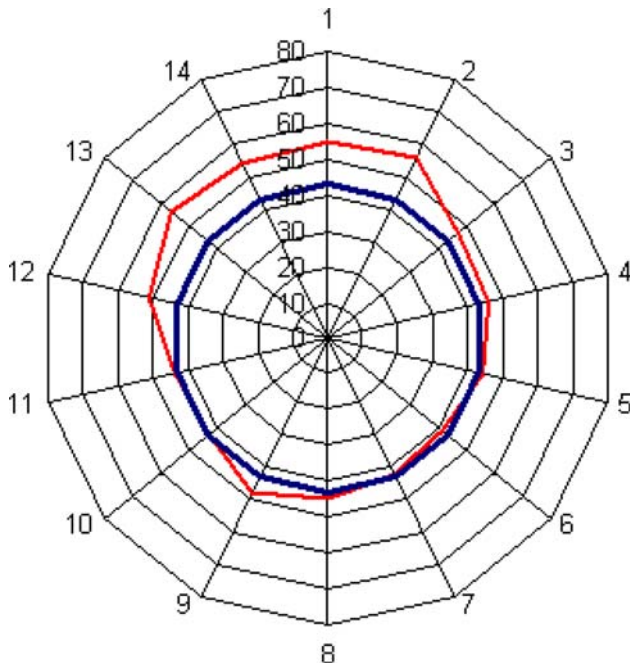

Fig. 7 Diagram showing the alpha angles in Group I that included hips with spherical contours on both the anteroposterior pelvis and lateral crosstable views. No signs of asphericity.

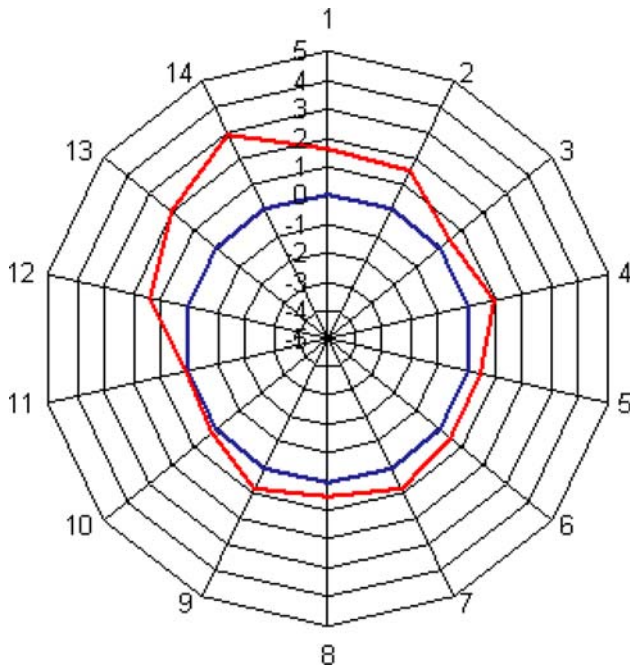

Fig. 8 Diagram showing the height of the asphericity in Group I that included hips with spherical contours on both the anteroposterior pelvis and lateral crosstable views. No signs of asphericity.

o'clock) (Table 1). The four hips in Group III showed a second peak inferiorly at 7 o'clock.

The asphericity was most distinctive in Group IV with 4.5 mm at the 12 o'clock position. In Group I with no

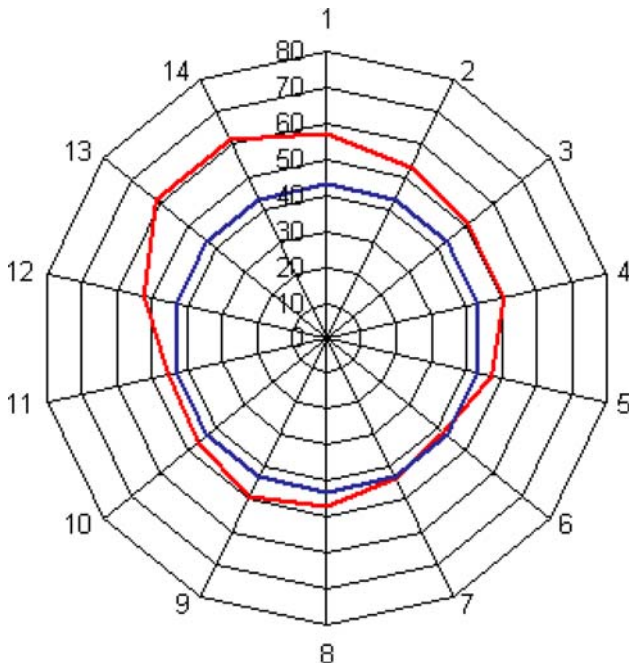

Fig. 9 Diagram showing the alpha angles in Group II that included hips with asphericity on the lateral crosstable view only.

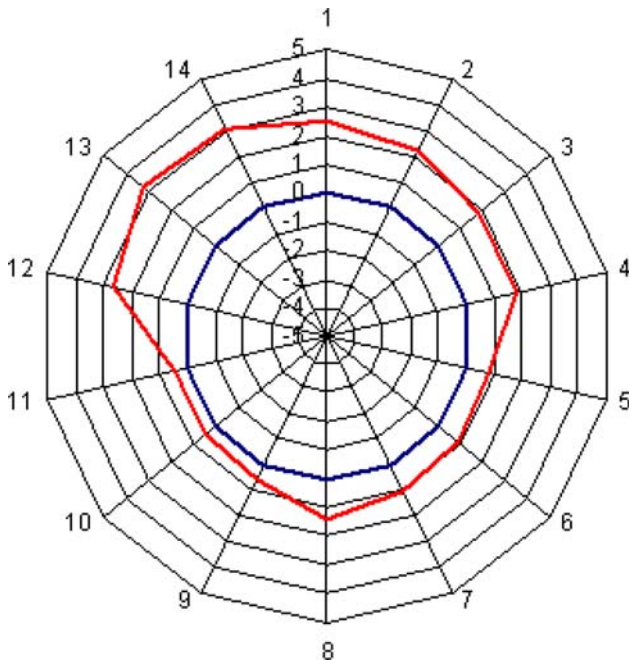

Fig. 10 Diagram showing the height of asphericity in Group II that included hips with asphericity on the lateral crosstable view only.

radiographic signs, the largest bump was at the 11 o'clock position with 2.8 mm. In Group II with only axial signs, it was 3.3 mm at the 10 o'clock position and in Group III the bump was 2.8 mm at the 10 o'clock position (Table 1).

In Group I, the alpha angle was maximally increased in Slice 13 with 56.2°, equivalent to the 10 o'clock position

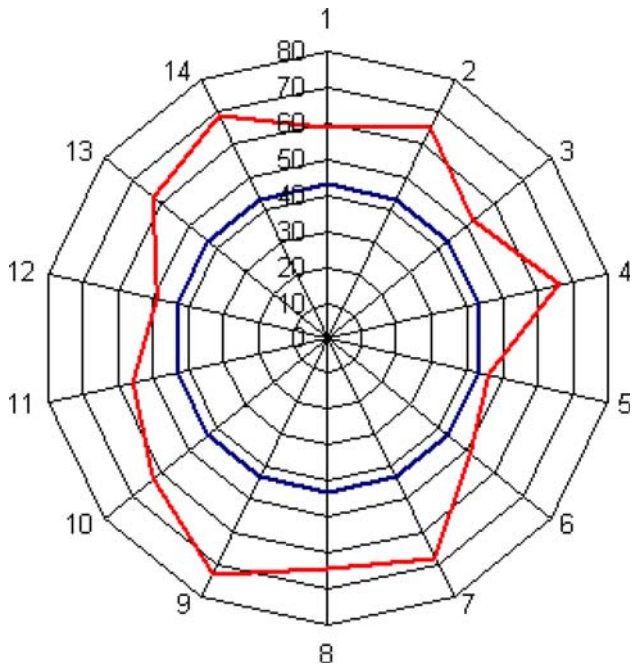

Fig. 11 Diagram showing the alpha angles in Group III that had asphericity of the hip on the anteroposterior pelvis (eg, pistol grip deformity) and normal contour in the lateral crosstable view.

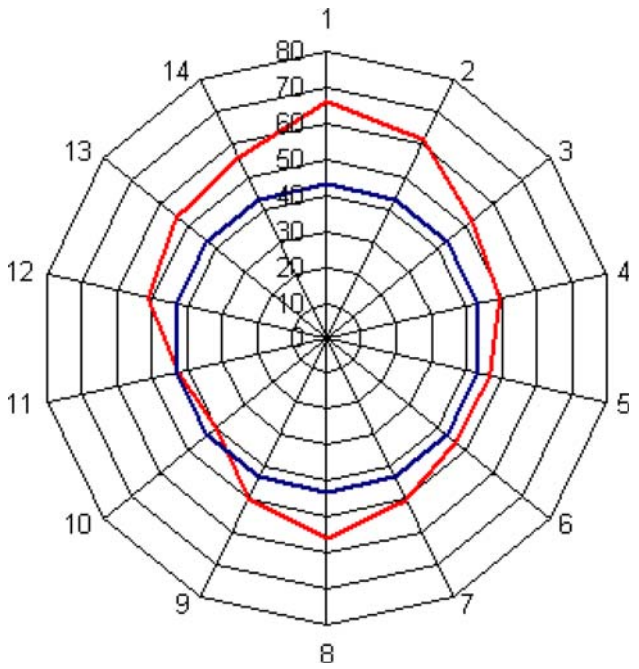

Fig. 13 Diagram showing alpha angles in Group IV that included hips with aspheric head-neck junction on both views.

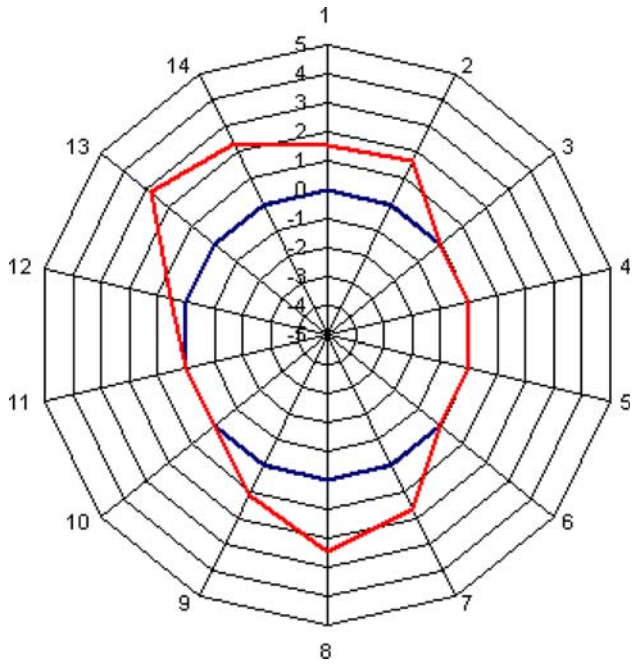

Fig. 12 Diagram showing the height of asphericity in Group III that had asphericity of the hip on the anteroposterior pelvis (eg, pistol grip deformity) and normal contour in the lateral crosstable view.

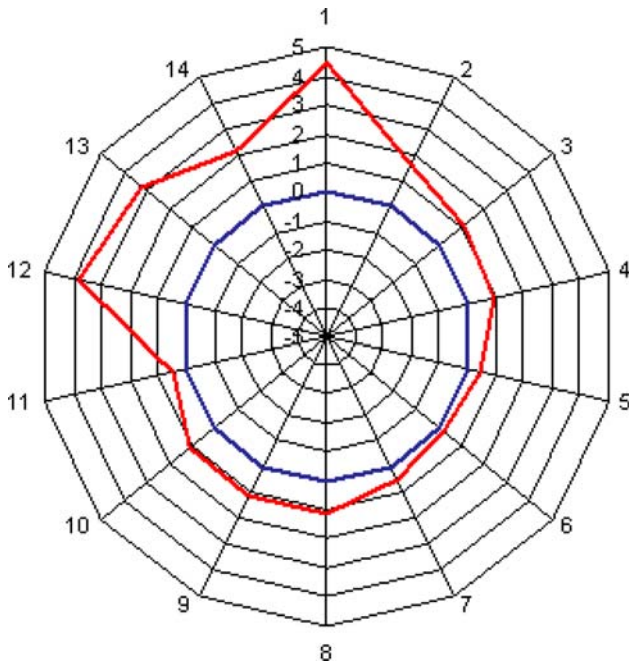

Fig. 14 Diagram showing the height of asphericity in Group IV that included hips with aspheric head-neck junction on both views.

(Fig. 7). The height of the asphericity measured 2.8 mm in Slice 14, equivalent to the 11 o'clock position (Fig. 8).

In Group II, the alpha angle was highest in Slice 14, equivalent to the 11 o'clock position with 61.4° (Fig. 9). The height of the asphericity averaged a maximum of 3.3 mm in Slice 13, equivalent to the 10 o'clock position (Fig. 10).

In Group III, the distribution of the alpha angles was heterogeneous. The highest alpha angle was in Slice 9,

equivalent to the 7 o'clock position with 73.1° and a second peak at Slice 14 (11 o'clock) with 69.2° (Fig. 11). The height of the asphericity measured 2.8 mm in Slice 13, equivalent to the 1 o'clock position and 2.5 mm at the 6 o'clock position (Fig. 12).

In Group IV, the highest alpha angle was 66.2° in Slice 1, equivalent to the 12 o'clock position (Fig. 13). The height of asphericity measured 4.5 mm in Slice 1, equivalent to the 12 o'clock position (Fig. 14).

Discussion

Asphericity of the femoral head-neck junction is one cause of FAI that can eventually lead to osteoarthrosis of the hip. The asphericity of the femoral head-neck junction is often underestimated [8]. To date, there are no studies that compare the accuracy of the visualization of the asphericity on conventional radiographs to the anatomic representation on MRA with radial slices. The aim of this study was to evaluate whether asphericity of the femoral head-neck junction can be missed or underestimated if standard radiographs are normal and whether MRA with radial slices is superior to regular radiographs to visualize osseous abnormalities.

A limitation of this study is the high dropout rate due to imaging that was not suitable for the study. It can be questioned if those additional 41 hips would have altered the results. Theoretically, the distribution of the four groups could be different, however, we believe the influence on the values of alpha angle and height of asphericity is less likely, given the reasonable number of hips in Groups I, II and IV. The interpretation of the results of Group III is limited by the small number that precludes statistical analysis with the calculation of mean values. Whether those hips really have an additional inferior decrease of the femoral head neck offset has to be examined by a larger group of such hips. Another limitation may be the possible bias caused by the referral system. Often patients referred from outside already have had their MRA and while the quality of these examinations did not meet the standards for this study they were sufficient for diagnosis and treatment. This was the case if the deformity causing FAI was large and visible on the standard radiographs. In these cases MRA was only used to assess the state of labral and acetabular cartilage damage. Because hips with subtle deformities rather had a repeat MRA with good quality this may have led to an overrepresentation of such hips in this study. Finally, the precision to match the axis of the radial slices perfectly to the axis of the femoral neck is within 1 to 2 mm. This will lead to an underestimation of the values of the alpha angle and height of asphericity because the measurements are not taken at the largest diameter but just next to it. If there is an error, then towards an underestimation of the true value.

Not surprisingly, the hips in Group IV with radiographic signs in both the anteroposterior and crosstable views had the highest alpha angle and also the most prominent asphericity. In all four groups, an asphericity of the head-neck junction was present on the anterosuperior aspect of the femoral head-neck junction. In group III high alpha angles were also measured inferiorly.

The results in Group I without radiographic signs of asphericity on standard radiographs are interesting. Even in this group, the alpha angle and the asphericity was increased in the anterosuperior region. All these patients would have been missed if diagnosis would have relied on standard radiographs only. For this group that accounts for 34.6% of the study population, it was important to have an additional examination not to overlook the asphericity and the resulting FAI.

Of the two pathomechanisms of FAI, cam impingement with the aspheric head-neck junction is the more important, because it leads early to extensive acetabular cartilage damage [2]. To assess the shape of the proximal femur, there is a need for an accurate tool to visualize asphericity. Conventional radiographs are not accurate enough to visualize the circumference of the femoral head-neck area of the proximal femur, especially in subtle deformities [16]. Different radiographic views and imaging techniques have been described to assess osseous deformities of the femoral head-neck junction, referring to standard views [4, 8, 17, 18]. However, a limitation of conventional radiographs always is that only the outline of the bones are clearly visualized. With MRA with radial slices this problem can be solved. Alternately, CT scans with 3-D reconstructions will also show the deformity accurately, but measurement of the alpha angle is more difficult to obtain [1]. In addition, concomitant lesions of the labrum and cartilage cannot be visualized as well [14, 26]. It is an advantage to assess the complete joint with only one examination to assess the deformities and secondary joint damages.

Of great importance is to understand that an aspheric head-neck junction does not necessarily indicate FAI. Motion of the hip depends on the shape of the head-neck junction and the shape of the acetabulum. In a hip with a dysplastic acetabulum asphericity will not cause FAI because the acetabulum is too small and maloriented to permit an abutment between these two joint components. On the other hand, in a deep or a retroverted acetabulum, overcoverage may be such that even in the presence of a normal head-neck junction FAI occurs. This study shows that normal radiographs do not allow the conclusion that the femoral head-neck junction is spherical. Therefore, in patients with clinical symptoms of FAI additional

investigations, best with MRA with radial slices, are necessary to rule out FAI.

It is important that the all radial slice planes include the axis of the femoral neck. Often radiologists offer radial slices through the femoral head along a longitudinal axis not coincident with that of the femoral neck. These radial slices are useless for mapping the outline of the femoral neck and cannot contribute to diagnosis and understanding of the pathomorphology. For diagnosing labral and joint cartilage abnormalities, radial slices are helpful but not necessary [28].

In the past, previous MR studies have focused on MRA to investigate soft tissue structures like labral and chondral impairments [9, 13, 14, 16]. However, only the radial slices can show the complete circumference of the bony structure of the proximal femur [10, 16, 26]. Using radial slices in 50 patients with MRA, Pfirrman et al. reported the largest alpha angles in cam FAI and pincer FAI appear in the anterior-superior position and they recommend radial slices [19]. The number of radial slices can be varied to focus on the most interesting parts of the joint [16].

MRA with radial slices in the axis of the femoral head neck is necessary to visualize the asphericity of the head-neck junction and to establish the diagnosis of cam FAI in modest deformities, which cannot be visualized with conventional radiographic techniques. Without correct imaging, asphericity of the head-neck junction would be underestimated in a high number of patients, 34.6% in this series.

Acknowledgments We thank Simon Steppacher, MD, Dept. of Orthopaedic Surgery, Inselspital, University of Berne, Switzerland and New England Baptist Hospital, Tufts University, Boston, USA and Moritz Tannast, MD, Dept. of Orthopaedic Surgery, Inselspital, University of Berne, Switzerland for help with the figures. Gert Muhr, MD, Professor of Surgery, Surgeon in Chief, Dept. of Surgery, University Hospital Bergmannsheil, Ruhr-University Bochum, Germany supported my Fellowships at Childrens Hospital Boston, Harvard Medical School, USA and Inselspital Berne, University of Berne, Switzerland.

References

1. Beaule PE, Zaragoza E, Motamedi K, Copelan N, Dorey FJ. Three-dimensional computed tomography of the hip in the assessment of femoroacetabular impingement. *J Orthop Res.* 2005;23:1286–1292.
2. Beck M, Kalhor M, Leunig M, Ganz R. Hip morphology influences the pattern of damage to the acetabular cartilage: femoroacetabular impingement as a cause of early osteoarthritis of the hip. *J Bone Joint Surg Br.* 2005;87:1012–1018.
3. Clohisy JC, Nunley RM, Otto RJ, Schoenecker PL. The frog-leg lateral radiograph accurately visualized hip cam impingement abnormalities. *Clin Orthop Relat Res.* 2007;462:115–121.
4. Eijer H, Leunig M, Mahomed M, Ganz R. Crosstable lateral radiograph for screening of anterior femoral head-neck offset in patients with femoroacetabular impingement. *Hip Int.* 2001;11:37–41.
5. Ganz R, Gill TJ, Gautier E, Ganz K, Krugel N, Berlemann U. Surgical dislocation of the adult hip a technique with full access to the femoral head and acetabulum without the risk of avascular necrosis. *J Bone Joint Surg Br.* 2001;83:1119–1124.
6. Ganz R, Parvizi J, Beck M, Leunig M, Notzli H, Siebenrock KA. Femoroacetabular impingement: a cause for osteoarthritis of the hip. *Clin Orthop Relat Res.* 2003;417:112–120.
7. Heyworth BE, Shindle MK, Voos JE, Rudzki JR, Kelly BT. Radiologic and intraoperative findings in revision hip arthroscopy. *Arthroscopy.* 2007;23:1295–1302.
8. Ito K, Minka MA, 2nd, Leunig M, Werlen S, Ganz R. Femoroacetabular impingement and the cam-effect. A MRI-based quantitative anatomical study of the femoral head-neck offset. *J Bone Joint Surg Br.* 2001;83:171–176.
9. Kassarjian A, Yoon LS, Belzile E, Connolly SA, Millis MB, Palmer WE. Triad of MR arthrographic findings in patients with cam-type femoroacetabular impingement. *Radiology.* 2005;236:588–592.
10. Kubo T, Horii M, Harada Y, Noguchi Y, Yutani Y, Ohashi H, Hachiya Y, Miyaoka H, Naruse S, Hirasawa Y. Radial-sequence magnetic resonance imaging in evaluation of acetabular labrum. *J Orthop Sci.* 1999;4:328–332.
11. Leunig M, Beck M, Woo A, Dora C, Kerboull M, Ganz R. Acetabular rim degeneration: a constant finding in the aged hip. *Clin Orthop Relat Res.* 2003;413:201–207.
12. Leunig M, Casillas MM, Hamlet M, Hersche O, Nötzli H, Slongo T, Ganz R. Slipped capital femoral epiphysis: early mechanical damage to the acetabular cartilage by a prominent femoral metaphysis. *Acta Orthop Scand.* 2000;71:370–375.
13. Leunig M, Podeszwa D, Beck M, Werlen S, Ganz R. Magnetic resonance arthrography of labral disorders in hips with dysplasia and impingement. *Clin Orthop Relat Res.* 2004;418:74–80.
14. Leunig M, Werlen S, Ungersbock A, Ito K, Ganz R. Evaluation of the acetabular labrum by MR arthrography. *J Bone Joint Surg Br.* 1997;79:230–234.
15. Locher S, Werlen S, Leunig M, Ganz R. Inadequate detectability of early stages of coxarthrosis with conventional roentgen images [in German]. *Z Orthop Ihre Grenzgeb.* 2001;139:70–74.
16. Locher S, Werlen S, Leunig M, Ganz R. MR-Arthrography with radial sequences for visualization of early hip pathology not visible on plain radiographs [in German]. *Z Orthop Ihre Grenzgeb.* 2002;140:52–57.
17. Meyer DC, Beck M, Ellis T, Ganz R, Leunig M. Comparison of six radiographic projections to assess femoral head/neck asphericity. *Clin Orthop Relat Res.* 2006;445:181–185.
18. Notzli HP, Wyss TF, Stoecklin CH, Schmid MR, Treiber K, Hodler J. The contour of the femoral head-neck junction as a predictor for the risk of anterior impingement. *J Bone Joint Surg Br.* 2002;84:556–560.
19. Pfirrmann CW, Mengiardi B, Dora C, Kalberer F, Zanetti M, Hodler J. Cam and pincer femoroacetabular impingement: characteristic MR arthrographic findings in 50 patients. *Radiology.* 2006;240:778–785.
20. Reynolds D, Lucas J, Klaue K. Retroversion of the acetabulum. A cause of hip pain. *J Bone Joint Surg Br.* 1999;81:281–288.
21. Siebenrock KA, Kalbermatten DF, Ganz R. Effect of pelvic tilt on acetabular retroversion: a study of pelves from cadavers. *Clin Orthop Relat Res.* 2003;407:241–248.
22. Siebenrock KA, Schoeniger R, Ganz R. Anterior femoro-acetabular impingement due to acetabular retroversion. Treatment with periacetabular osteotomy. *J Bone Joint Surg Am.* 2003;85:278–286.
23. Siebenrock KA, Wahab KH, Werlen S, Kalhor M, Leunig M, Ganz R. Abnormal extension of the femoral head epiphysis as a cause of cam impingement. *Clin Orthop Relat Res.* 2004;418:54–60.

24. Tönnis D. *Congenital Dysplasia and Dislocation of the Hip in Children and Adults*. New York, NY: Springer; 1987.
25. Tönnis D. Normal values of the hip joint for the evaluation of X-rays in children and adults. *Clin Orthop Relat Res.* 1976;119:39–47.
26. Werlen S, Leunig M, Ganz R. Magnetic Resonance Arthrography of the hip in femoroacetabular impingement: technique and findings. *Oper Tech Orthop.* 2005;15:191–203.
27. Wiberg G. Studies on dysplastic acetabula and congenital subluxation of the hip joint. With special reference to the complications of osteoarthitis. *Acta Chirurgica Scandinavica.* 1939;58(Suppl):5–135.
28. Yoon LS, Palmer WE, Kassarjian A. Evaluation of radial-sequence imaging in detecting acetabular labral tears at hip MR arthrography. *Skeletal Radiol.* 2007;36:1029–1033.